Polymer Chemistry

Accepted Manuscript

ROYAL SOCIETY OF CHEMISTRY

www.rsc.org/polymers

Polymer Chemistry

Polymer Chemistry

Dynamic Article Links►

Cite this: DOI: 10.1039/c0xx00000x

ARTICLE TYPE

www.rsc.org/xxxxxx

Morphology-Controlled Dual Clickable Nanoparticles via Ultrasonic-Assisted Click Polymerization

Yong Hou,[a] Shoupeng Cao,[a] Lin Wang,[a] Yuxin Pei,*[a] Guoyun Zhang,[a] Siwen Zhang [b] and Zhichao Pei*[a]

Received (in XXX, XXX) XthXXXXXXXXX 20XX, Accepted Xth XXXXXXXXX 20XX

DOI: 10.1039/b000000x

Morphology-controlled dual clickable nanoparticles (DCNPs) were synthesized in one step via ultrasonic-assisted azide-alkyne click polymerization. The morphology of DCNPs was strongly dependent on solvent and co-monomer structure. Numerous unreacted alkynyl and azido groups on the surface of DCNPs facilitated the nanocarrier platforms for further functionalization via click chemistry.

Functional polymeric nanoparticles have been recognized as an efficient tool for cell imaging,[1] drug delivery,[2,3] bioanalysis,[4] and other biological areas.[5-7] Recent studies have shown that the behaviour and properties of NPs are strongly influenced by their morphology.[8,9] For instance, rod-shaped nanoparticles (NPs) exhibit higher specific and lower non-specific accumulation on endothelial cells compared to their spherical counterparts.[10] Mammalian cell uptake of NPs is particle-shape dependent: disc-shaped NPs are internalized more efficiently than rod-shaped NPs.[11] It is therefore of great importance to develop approaches for controlling the precise geometry of NPs.[12,13] The approaches reported so far include indirect strategies based on performed polymers, such as microfluidic platform for precise control of sub-100 nm polymeric NPs based on polybenzimidazole from spherical to elliptical,[12] and direct strategies (so-called monomer-to-nanoparticle) such as one-pot synthesis of branched amphiphilic block copolymers for dumbbell and tripartite organic NPs.[14,15]

Bi- or multi-functional NPs are emerging as useful tools for many biological applications due to their ability to facilitate the assembly of multiple components onto a single nanocarrier platform.[16,17] In this regard, the multifunctional worms and rods were synthesized by using RAFT-mediated dispersion polymerization,[16] the alkynyl/azide dual surface-functionalized nanogels prepared by inverse emulsion method,[18] and the carboxyl/hydroxyl dual surface-functionalized polystryrene/Fe_3O_4@SiO_2 Janus NPs prepared by miniemulsification method.[19] However, the methods require a relatively large amount of surfactants, which are irremovable from nanoparticle surfaces in many cases.[20] These residues, especially fluorinated surfactants, on the surface of nanoparticles are undesirable for many applications including cell imaging and drug delivery. The drawbacks are not only high cytotoxicity[21,22] caused by the surfactants themselves, but also the possible blocking of access to the modified surfaces.[23] Thus, development of surfactant-free approaches for fabricating bi- or multi-functional NPs is highly desired. To this day, no known method represents a direct monomer-to-nanoparticle synthesis with consideration of both morphology control and dual surface functionalization of NPs.

Here we report a novel synthetic approach for direct monomer-to-nanoparticle synthesis of morphology-controlled DCNPs in one step via ultrasonic-assisted alkyne-azide click polymerization catalyzed by $Cu(PPh_3)_3Br$, avoiding the need of surfactants. The morphology of DCNPs (spherical or rod-like) was strongly dependent on solvent and co-monomer structure under ultrasonic irradiation. The monomers and co-monomers used for click polymerization in this work are listed in Scheme 1.

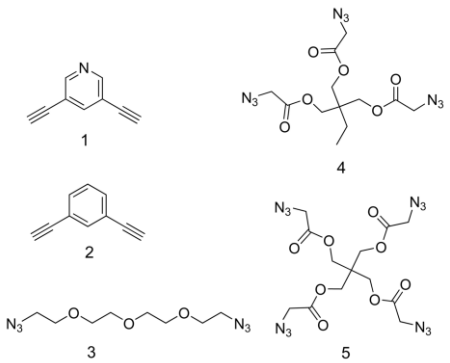

Scheme 1 The chemical structures of monomers (**1-2**) and co-monomers (**3-5**) used for the synthesis of DCNPs

To fabricate DCNPs via click polymerization, 3,5-diethynylpyridine (**1**) and 1,3-diethynylbenzene (**2**) were chosen as monomers. The 6-member ring of the monomers along with the triazole rings formed during azide-alkyne polymerization endowed the nanoparticles essential structural rigidity. 1-azido-2-(2-(2-(2-azidoethoxy)ethoxy)ethoxy)ethane (di-azide, **3**), 1,3-bis(azidoacetoxy)-2-azidoacetoxymethyl-2-ethylpropane (tri-azide, **4**), and 2,2-bis((2-azidoacetoxy)methyl)propane-1,3-diyl bis(2-azidoacetate) (tetra-azide, **5**) were used as co-monomers. The alkyne-azide cycloaddition between either of the monomers

and any of the co-monomers, six "monomer + co-monomer" combinations in total were catalyzed by $Cu(PPh_3)_3Br$, which is more effective due to its good solubility in organic solvents.[22] To overcome aggregation among NPs resulting from their high surface energy (Fig. S1), ultrasonic irradiation (40 kHz) was used for all of the polymerizations. The adhesion of nanoparticles was restrained by the mechanical force or so-called cavitation effect arised from ultrasonic irradiation,[24] thus avoiding the need of surfactants.

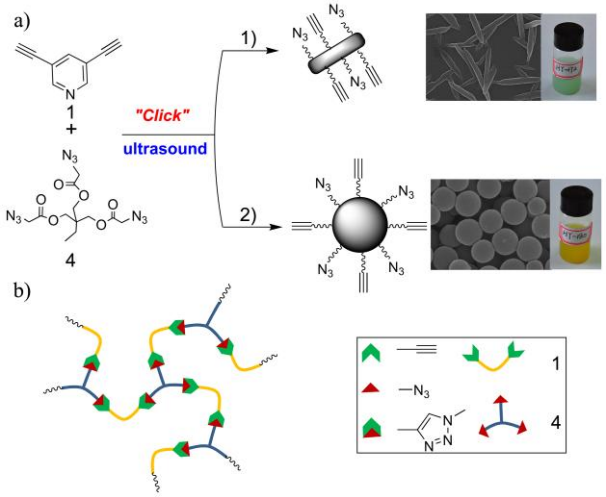

Scheme 2 Schematic diagram illustrating the ultrasonic assisted synthesis of DCNPs with monomer **1** and co-monomer **4**: (a) 1) $CHCl_3$, nanorods; 2) $CH_3CN/CHCl_3$ (96:4, v/ve), nanoshperes. (b) Schematic diagram illustrating the structure of crosslinked DCNPs.

To control the morphology of DCNPs, we first studied the effect of solvents because of its crucial impact.[25] Our investigation reinforced the idea that the morphology is strongly solvent dependent. By taking the polymerization between **1** and **4** as an example (Scheme 2), it can be clearly seen that the morphology of DCNPs formed in different solvents varied and could be controlled satisfactorily by choosing suitable solvent system: Polymerization performed in chloroform induced formation of nanorods (dual clickable nanorod, DCNR), appearing as a green emulsion (Fig. 1a, Scheme 2a1), whereas a change of solvent to 4 vol. % chloroform in CH_3CN induced formation of nanospheres (dual clickable nanosphere, DCNS), appearing as a yellow emulsion (Fig. 1b, Scheme 2a2); Additionally, slightly adhesive nanospheres with minor distortions in dichloromethane (DCM, Fig. 1c) and irregular NPs with heavy adhesion in tetrahydrofuran (THF) were obtained (Fig. 1d). Noticing the completely different morphologies of DCNPs formed in $CHCl_3$ and DCM, the effect of the mixture of $CHCl_3$ and DCM at different ratios on the morphology was further investigated. The results showed that 80-100 % of $CHCl_3$ is necessary to assure the formation of nanorods (Fig. S2a and S2b). A decrease of the ratio to 70 % resulted in amorphous particles (Fig. S2c).

To thoroughly understand the essential requirements for controlling morphology, further studies focused on influence of the structures of the monomers and co-monomers. It was found that, 1) when 3,5-diethynylpyridine was used as monomer, only nanorods could be obtained with di-azide linear co-monomer **3** (Fig. 2a), while only nanospheres could be produced with symmetric tetra-azide co-monomer **5** (Fig. 2b). However, both nanorods and nanospheres could be prepared with tri-azide co-monomer **4** under suitable conditions (Fig. 1a and 1b); 2) when 1,3-diethynylbenzene **2** was used instead of **1** as monomer, the polymerizations were sluggish. The temperature had to be increased to 20 ℃ along with a prolongation of reaction to 5 h to form precipitate. As a matter of fact, no precipitate was obtained with di-azide **3** even under these conditions. In a word, spherical particles from nanon to micron scales could be obtained when **2** was used instead of **1** (Fig. 3b and 3c). However, polymerization of **2** with tri-azide **4** could not lead to nanorod formation under the same conditions that worked for **1**, but instead led to the aggregation of irregular nanoparticles (Fig. 3a).

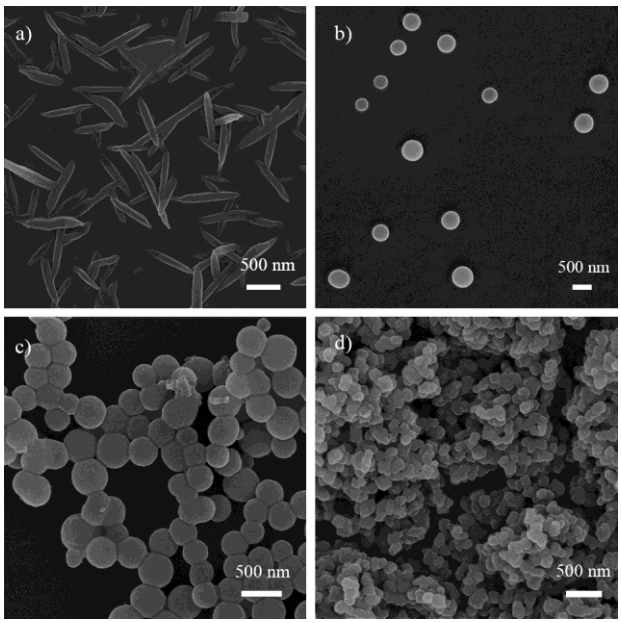

Fig. 1 FESEM images of DCNPs synthesized from **1** + **4** combination under ultrasonic irradiation: (a) $CHCl_3$; (b) $CH_3CN/CHCl_3$ (96:4, v/v); (c) DCM; (d) THF.

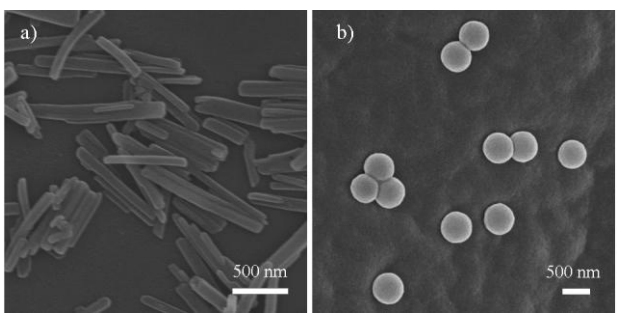

Fig. 2 FESEM images of DCNPs synthesized from different "monomer + co-monomer" combinations under ultrasonic irradiation: (a) **1** + **3**; (b) **1** + **5**.

On the whole, these results implied that, in addition solvent, structures of monomer/co-monomer are the other decisive factor for manipulating morphology. The final morphology of nanoparticles was strongly dependent on both solvent and structures of monomer/co-monomer and is ultimately decided by

their synergetic effect.

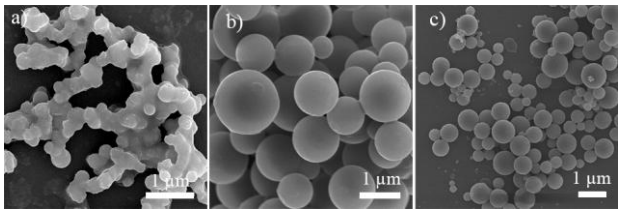

Fig. 3 FESEM images of the nanoparticles synthesized by 1,3-diethynylbenzene under ultrasonic with different co-monomers in different solvents, 5 h, 20 ℃. (a) **2** + **4**, $CHCl_3$; (b) **2** + **4**, $CH_3CN/CHCl_3$ (96:4, v/v); (c) **2** + **5**, $CH_3CN/CHCl_3$ (96:4, v/v).

Interestingly, nanorods could only be obtained when 3,5-diethynylpyridine was used as monomer, while no rod-like NPs could be produced with **2**. The lacking of the N atom in the benzene ring in 1,3-diethynylbenzene is the only difference between the monomers, we thus deduce that the Nitrogen atom on the pyridine ring is crucial for the formation of nanorods. Along with the green color of the nanorod emulsion, we believe that there is a coordination of N atoms on the pyridine rings to copper ions, and is the major driving force for the alignment of linear polymer chain (from **1** + **3**) or low branched polymer chain (from **1** + **4**) along the chain axial direction to form a bundle of polymers, which are the nanorods. Since nanorods are more crystalline than nanospheres, the failure to obtain nanorods in the **1** + **5** combination might be ascribed to the difficulty of the resulting polymer chains to align into highly oriented polymer chain bundles due to the hyperbranched structures.

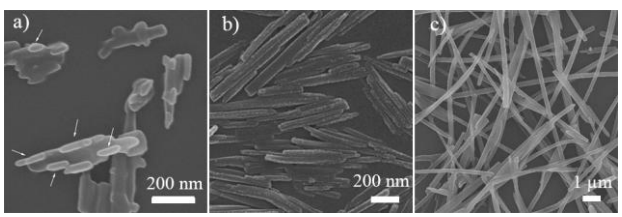

Fig. 4 FESEM images of rod-like polymers synthesized by **1** + **4** under ultrasonic in $CHCl_3$ for different time. a) 1.5 h; b) 2.5 h; c) 5 days.

If the surmise is true, we should find higher amount of copper ions on the surface of DCNRs than that on DCNSs. The analysis of XPS showed that the residual copper ions on the surfaces of DCNRs were 1.59 % (Fig. S3a), and on the surfaces of DCNSs were 0.55 % (Fig. S3b), which confirmed our conjecture.

On the other hand, with all the results in hand, we speculate that chloroform somehow aid the arrangement of N atom coordination with copper ions, which is another critical condition for rod formation, exemplified by monomer **2**. Without the coordination between N atoms and copper ions, the highly crosslinked polymers would be synthesized in a spherical shape. This fact may be derived from the polarity, dielectric constant, viscosity, and surface tension of the solvents.

In order to explore the mechanism of the growth of nanorods, the time-dependent experiment was carried out. SEM images obtained after different reaction times were shown in Fig. 4. With ultrasound treatment of 1.5 h, small primary rod-like particles or "nanorod seeds" (marked with arrows in Fig. 4a) were observed, which further aggregated in specific orientation and spontaneously attached on the backbone of the spindles to form rods-like structure (Fig. 4a). The length of the rods reached 1 μm after 2.5 h (Fig. 4b). After keeping the green emulsion at room temperature for 5 days, 10-20 μm long rods were obtained (Fig. 4c). Based on this interesting finding, we inferred that rod-like polymer seeds were formed under ultrasonic irradiation in chloroform.

To prove the existence of the "seeds", 2.5 mL aliquot supernatant of the reaction mixture was obtained by centrifugation and dried, then the residue containing unreacted monomer, co-monomer, and catalyst was redissolved into 1 mL chloroform, DMF, THF, and DCM, respectively. After keeping the solutions at room temperature for 3 days, the rod polymers were obtained with all of the four solvents (see Fig. S4), indicating once the rod-like seeds formed in chloroform by ultrasonication, they can grow along the axial direction of the seeds into rods of several micrometers not only in chloroform, but also in other different solvents. It seems that the seeds only form in chloroform, the change of solvent leads to the growth of the rod polymer while preserving the rod-like structure of the seeds. The similar phenomenon was reported by Winnik and co-workers.[26]

In contrast, "the seed effect" was not observed when a similar process was repeated with the supernatant from Entry 3 in Table S1, where spherical shape of particles was not maintained in more polar solvents, such as DMF and THF, while better spheres were obtained in DCM (Fig. S5).

Additionally, many other reaction conditions have been investigated included: 1) Temperature: The reaction was very sluggish if the temperature was lower than 6-8 ℃, while heavy aggregation occured if the temperature exceeded 20 ℃. The optimal range was concluded to be 10-15 ℃. 2) Concentrations of monomers: its effect on the synthesis of DCNPs was investigated with three different concentrations of 0.03, 0.12, and 0.24 M. For DCNSs, higher concentrations caused heavy aggregation (Fig S6a-c); while for DCNRs, concentration had little effect on the morphology but did have a slight impact on the reaction rate (Fig S6d-f). 3) Frequency: it is one of the crucial conditions for the formation of nanorods, where the increase in frequency to 80 kHz, for instance, gave no fomation of nanorods, while the nanoshperes formed had a wider polydispersity and heavier aggregation in comparison with that at 40 kHz (Fig S7). 4) Power of ultrasonic: the investigation on the effect of the power of ultrasonic irradiation on the morphology revealed that its main effect on nanospheres is on their size as well as the polydispersity, but not their shape (Fig. S8a-c). In contrast, the power did have an effect on the shape of nanorods, which could only be formed under the highest ultrasonic power of 300 W (Fig S8d-f).

Besides field emission scanning electron microscope (FESEM), the corresponding DCNPs were characterized by FTIR, X-ray diffraction (XRD), as well as dynamic light scattering (DLS, Table S1 and Fig. S9). The IR spectra of DCNR and DCNS were shown in Fig. 5a. The stretching vibrations of C-H, C≡C in propargyl and azide group on the surface of DCNPs were

observed at 3245 cm^{-1}, 2106 cm^{-1}, and 2097 cm^{-1}, respectively. The curves of XRD were shown in Fig. 5b, where many sharp reflections with a 2θ range from 5 ° to 35 ° for DCNR and a very broad reflection centered with 2θ = 23 ° for DCNS were observed. The difference in XRD showed that the nanorods were more crystalline than the nanospheres, which pointed to completely different processes during NP formation. There was almost no order being formed in the case of the spheres in $CH_3CN/CHCl_3$ mixture, whereas the rods with high orientation formed in $CHCl_3$. The DLS analysis displayed that the mean size of DCNSs was 674 ± 72 nm with PDI (polydispersity index) of 0.392. The average aspect ratio of DCNR was 7.1. The amount of azide and alkynyl groups on the surface of DCNPs could be determined by HPLC, take DCNSs from **1** + **4** as an example, the amount of azide groups was 38 μmol/g polymer, and that of alkynyl groups was 15 μmol/g polymer (Fig. S10).

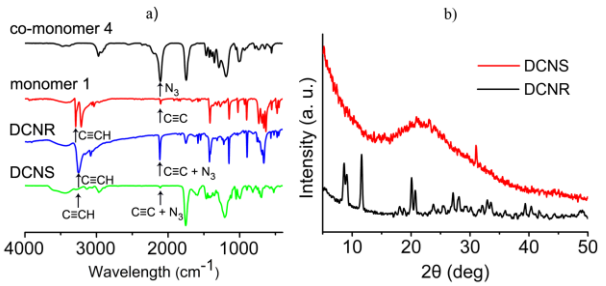

Fig. 5 The IR (a) and XRD (b) spectra of DCNS and DCNR.

Moreover, we believe that DCNRs have a lower degree of polymerization than DCNSs based on three evidences: the appearance, solubility, and thermostability of DCNPs. 1) The appearance: DCNRs are more crystalline than DCNSs; 2) Solubility: DCNRs can be dissolved in DMSO by ultrasonication, DCNSs can not; 3) Thermostability: Thermal gravity analysis (TGA) showed that DCNRs experienced two stages of weight loss, 45.26 % weight loss at about 181.76 ℃ and further 38.35 % weight loss at about 436.2 ℃ (Fig. S11a). The first loss possibly corresponded to the breakage of coordination bonds formed by N atoms on the pyridine rings with copper ions and the hydrogen bonds formed among polymer chains due to a large numbers of N atoms in the triaole rings and O atoms from the co-monomers; while the second loss corresponded to the breakage of covalent bonds of the polymer chains. For DCNSs, only one stage of weight loss of 60.40 % at 322.51 ℃ was observed (Fig. S11b), which was attributed to the breakage of covalent bonds of highly crosslinked DCNSs.[27]

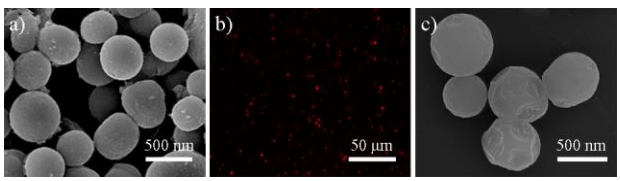

Fig. 6 The FESEM (a) and LSCM (b) images of fluorescent glyconanopaticles (FGNPs) and the FESEM image (c) of glyconanopaticles (GNPs).

To exemplify the potential of DCNPs as nanocarrier platforms for facilitating further conjugation of multiple molecules or ligands, fluorescent glyconanopaticles (FGNPs) were fabricated. Fluorescence labelling, despite its many advantages, may affect the bioactivities of directly labelled biomolecules.[28] With DCNPs synthesized in this work, we can conveniently combine multivalent fluorescent labels and biomolecules (such as carbohydrates) in one single nanocarrier platform, avoiding direct labelling on the biomolecules. Here, FGNPs were fabricated by clicking with azide-tagged Rhodamine B (**8**) and alkyne-tagged lactose (**6**) sequentially (chemical structures see in Scheme S1). After modification, the IR characteristic absorption peaks of alkynyl and azide groups disappeared and a very broad absorption peak range from 3755 cm^{-1} to 3134 cm^{-1} from hydroxyl groups in lactose appeared (Fig. S12). Moreover, the surface of the NPs became slightly rough (Fig. 6a). The FGNPs could be observed by the laser scanning confocal microscope (LSCM) (Fig. 6b), which indicated that the modification was successful.

The analysis of XPS (Fig. S3) showed that the residual copper ions on the surface of were 1.59 % for DCNRs, and 0.55 % for DCNSs. Thus a concern regarding the toxicity of residual copper ions in DCNPs when applied in the area of biomedicine arises. Therefore, additional cytotoxicity studies on HeLa cells with glyconanoparticles (GNPs, Fig. 6c) synthesized from DCNSs, by conjugating lactose via click reaction with clickable lactoses of **6** and **7** onto their surfaces (Fig. S13), have been performed. Delightfully, no obvious apoptosis was found even after 48 h co-incubation of the cells with GNPs (Fig. S14), which proves that DCNPs synthesized with our approach can be a facile nanocarrier platform for further constructing functionalized bioconjugates.

In conclusion, morphology-controlled DCNPs were synthesized for the first time via ultrasonic-assisted azide-alkyne click polymerization in one step, avoiding the use of surfactant. The morphology of DCNPs (nanosphere or nanorod) can be well controlled by choosing suitable monomer, co-monomer, and solvent with assistance of ultrasonic. It was found that the N atom on the pyridine ring of monomer 3,5-diethynylpyridine **1** is one of the critical factors to form the rod-like structure, where co-monomers either di-azide **3** or tri-azide **4** with **1** could induce formation of nanorods. Most interestingly, both nanorods and nanospheres could be prepared with the combination of tri-azide **4** and **1** under suitable conditions. Moreover, mechanism study indicated that the rodlike seeds only form in chloroform, which is a key to induce nanorods. Numerous terminal alkynyl and azide groups on the surface of DCNPs facilitate them being used as nanocarrier platforms for further conjugation of multiple molecules or ligands under mild conditions via click chemistry, which has been illustrated by the synthesis of FGNPs and GNPs via dual click reaction. Consequently, the properties of DCNPs, such as hydrophilicity and biocompatibility, will change according to the properties of conjugated molecules. Furthermore, the fluorescent tags can be replaced with other ligands, such as drugs, to conjugate to DCNPs for constructing carbohydrate-targeting drug delivery systems. We envision that this novel approach may be expanded to synthesize other polymer nanoparticles. DCNPs fabricated with our method may have

potential in cell biology and biomedicine, which is in fact currently being carried out in our laboratory.

We thank the National Natural Science Foundation of China for financial support (NSFC21174113 and NSFC31270861). The authors also thank Mr. Yihan Pei from Clare College, University of Cambridge for the help with language.

Notes and references

[a] *Address, State Key Laboratory of Crop Stress Biology for Arid Areas and College of Science, Northwest A&F University, Yangling, Shaanxi 712100, People's Republic of China, Fax: +86 2987092769; Tel: +86 2987091196; E-mail: peiyx@nwafu.edu.cn; peizc@nwafu.edu.cn*
[b] *College of Chemistry, Northeast Normal University, Changchun, Liaoning 130024, People's Republic of China*

† Electronic Supplementary Information (ESI) available: Experimental procedures and additional results including FESEM images, XPS curves, DLS data, TGA thermograms, FTIR spectra, and cytotoxicity data. See DOI: 10.1039/b000000x/

1 X. Zhang, X. Zhang, B. Yang, Y. Zhang and Y. Wei, *ACS Appl. Mater. Interfaces.*, 2014, **6**, 3600.
2 Z. Zhao, H. Meng, N. Wang, M. J. Donovan, T. Fu, M. You, Z. Chen, X. Zhang and W. Tan, *Angew. Chem. Int. Ed.*, 2013, **52**, 7487.
3 W. Wu, Q. Zhang, J. Wang, M. Chen, S. Li, Z. Lin and J. Li, *Polym. Chem.*, 2014, **5**, 5668.
4 X. Lin, L. Cui, Y. Huang, Y. Lin, Y. Xie, Z. Zhu, B. Yin, X. Chen and C. J. Yang, *Chem. Commun*., 2014, **50**, 7646.
5 L. S. Lawson, J. W. Chan and T. Huser, *Nanoscale*, 2014, **6**, 7971.
6 E. C. Wang and A. Z. Wang, *Integr. Biol. (Camb)*., 2014, **6**, 9.
7 Y. X. Wu, J. B. Li, L. H. Liang, D. Q. Lu, J. Zhang, G. J. Mao, L. Y. Zhou, X. B. Zhang, W. Tan, G. L. Shen and R. Q. Yu, *Chem. Commun.*, 2014, **50**, 2040.
8 S. Barua, J.-W. Yoo, P. Kolhar, A. Wakankar, Y. R. Gokarn and S. Mitragotri, *Proc. Natl. Acad. Sci. U S A.*, 2013, **110**, 3270.
9 C. J. Yang and F. H. Lu, *Langmuir*, 2013, **29**, 16025.
10 P. Kolhar, A. C. Anselmo, V. Gupta, K. Pant, B. Prabhakarpandian, E. Ruoslahti and S. Mitragotri, *Proc. Natl. Acad. Sci. U S A.*, 2013, **110**, 10753.
11 R. Agarwal, V. Singh, P. Jurney, L. Shi, S. V. Sreenivasan and K. Roy, *Proc. Natl .Acad. Sci. U S A.*, 2013, **110**, 17247.
12 M. M. Hasani-Sadrabadi, F. S. Majedi, J. J. VanDersarl, E. Dashtimoghadam, S. R. Ghaffarian, A. Bertsch, H. Moaddel and P. Renaud, *J. Am. Chem. Soc.*, 2012, **134**, 18904.
13 S. Renker, S. Mahajan, D. T. Babski, I. Schnell, A. Jain, J. Gutmann, Y. Zhang, S. M. Gruner, H. W. Spiess and U. Wiesner, *Macromol. Chem. Phys.*, 2004, **205**, 1021.
14 T. He, D. J. Adams, M. F. Butler, A. I. Cooper and S. P. Rannard, *J. Am. Chem. Soc.*, 2009, **131**, 1495.
15 T. He, D. J. Adams, M. F. Butler, C. T. Yeoh, A. I. Cooper and S. P. Rannard, *Angew. Chem. Int. Ed.*, 2007, **46**, 9243.
16 Z. Jia, V. A. Bobrin, N. P. Truong, M. Gillard and M. J. Monteiro, *J. Am. Chem. Soc.*, 2014, **136**, 5824.
17 Y. Zhang, J. He, D. Cao, M. Zhang and P. Ni, *Polym. Chem.*, 2014, **5**, 5124.
18 D. A. Heller, Y. Levi, J. M. Pelet, J. C. Doloff, J. Wallas, G. W. Pratt, S. Jiang, G. Sahay, A. Schroeder, J. E. Schroeder, Y. Chyan, C. Zurenko, W. Querbes, M. Manzano, D. S. Kohane, R. Langer and D. G. Anderson, *Adv. Mater.*, 2013, **25**, 1449
19 F. Wang, G. M. Pauletti, J. Wang, J. Zhang, R. C. Ewing, Y. Wang and D. Shi, *Adv. Mater*., 2013, **25**, 3485.
20 B. J. Nehilla, P. G. Allen and T. A. Desai, *ACS Nano*, 2008, **2**, 538.
21 X. Zhang, M. R. Servos and J. Liu, *J. Am. Chem. Soc.*, 2012, **134**, 7266.
22 Y.-S. Lin and C. L. Haynes, *J. Am. Chem. Soc.*, 2010, **132**, 4834.
23 H. Chen, D. Wang, Y. Yu, K. A. Newton, D. A. Muller, H. Abruna and F. J. DiSalvo, *J. Am. Chem. Soc.*, 2012, **134**, 18453.
24 K. Nakabayashi, F. Amemiya, T. Fuchigami, K. Machida, S. Takeda, K. Tamamitsu and M. Atobe, *Chem. Commun*., 2011, **47**, 5765.
25 A. Kedia and P. S. Kumar, *J. Phys. Chem. C*., 2012, **116**, 23721.
26 X. Wang, G. Guerin, H. Wang, Y. Wang, I. Manners and M. A. Winnik, *Science*, 2007, **317**, 644.
27 A. Qin, C. K. W. Jim, W. Lu, J. W. Y. Lam, M. Häussler, Y. Dong, H. H. Y. Sung, I. D. Williams, G. K. L. Wong and B. Z. Tang, *Macromolecules*, 2007, **40**, 2308.
28 R. Alford, H. M. Simpson, J. Duberman, G. C. Hill, M. Ogawa, C. Regino, H. Kobayashi and P. L. Choyke, *Mol. Imaging*, 2009, **8**, 341.